

# Transplant of Autologous Mesenchymal Stem Cells Halts Fatty Atrophy of Detached Rotator Cuff Muscle After Tendon Repair

## Molecular, Microscopic, and Macroscopic Results From an Ovine Model

Martin Flück,<sup>\*‡</sup> PhD , Prof., Stephanie Kasper,<sup>‡</sup> PhD, Mario C. Benn,<sup>§</sup> DMV, DSc, Flurina Clement Frey,<sup>§</sup> PhD, Brigitte von Rechenberg,<sup>§</sup> DMV, Prof. Emeritus, Marie-Noëlle Giraud,<sup>||</sup> PhD, Dominik C. Meyer,<sup>†‡¶</sup> MD, Prof., Karl Wieser,<sup>¶</sup> MD, and Christian Gerber,<sup>¶</sup> MD , Prof. Emeritus

*Investigation performed at University of Zurich, Zurich, Switzerland*

**Background:** The injection of mesenchymal stem cells (MSCs) mitigates fat accumulation in released rotator cuff muscle after tendon repair in rodents.

**Purpose:** To investigate whether the injection of autologous MSCs halts muscle-to-fat conversion after tendon repair in a large animal model for rotator cuff tendon release via regional effects on extracellular fat tissue and muscle fiber regeneration.

**Study Design:** Controlled laboratory study.

**Methods:** Infraspinatus (ISP) muscles of the right shoulder of Swiss Alpine sheep ( $n = 14$ ) were released by osteotomy and reattached 16 weeks later without (group T;  $n = 6$ ) or with (group T-MSC;  $n = 8$ ) electropulse-assisted injection of 0.9 Mio fluorescently labeled MSCs as microtissues with media in demarcated regions; animals were allowed 6 weeks of recovery. ISP volume and composition were documented with computed tomography and magnetic resonance imaging. Area percentages of muscle fiber types, fat, extracellular ground substance, and fluorescence-positive tissue; mean cross-sectional area (MCSA) of muscle fibers; and expression of myogenic (myogenin), regeneration (tenascin-C), and adipogenic markers (peroxisome proliferator-activated receptor gamma [PPARG2]) were quantified in injected and noninjected regions after recovery.

**Results:** At 16 weeks after tendon release, the ISP volume was reduced and the fat fraction of ISP muscle was increased in group T (137 vs 185 mL; 49% vs 7%) and group T-MSC (130 vs 166 mL; 53% vs 10%). In group T-MSC versus group T, changes during recovery after tendon reattachment were abrogated for fat-free mass (−5% vs −29%, respectively;  $P = .018$ ) and fat fraction (+1% vs +24%, respectively;  $P = .009\%$ ). The area percentage of fat was lower (9% vs 20%;  $P = .018$ ) and the percentage of the extracellular ground substance was higher (26% vs 20%;  $P = .007$ ) in the noninjected ISP region for group T-MSC versus group T, respectively. Regionally, MCS injection increased tenascin-C levels (+59%) and the water fraction, maintaining the reduced PPARG2 levels but not the 29% increased fiber MCSA, with media injection.

**Conclusion:** In a sheep model, injection of autologous MSCs in degenerated rotator cuff muscle halted muscle-to-fat conversion during recovery from tendon repair by preserving fat-free mass in association with extracellular reactions and stopping adjuvant-induced muscle fiber hypertrophy.

**Clinical Relevance:** A relatively small dose of MSCs is therapeutically effective to halt fatty atrophy in a large animal model.

**Keywords:** rotator cuff; atrophy; fat; stem cell therapy; extracellular matrix; cell/molecular biology

Pluripotent mesenchymal stem cells (MSCs) have attracted considerable interest as biological agents to prevent muscle and tendon degeneration.<sup>25,26,38</sup> Especially for muscle

tissue, MSCs may mitigate fatty atrophy by enhancing the regenerative potential of muscle fiber-associated stem cell pools, such as satellite cells, that serve as reservoirs for development and regrowth of muscle fibers.<sup>31,34,40</sup> Because autologous MSCs are easily accessible and have a considerable capacity for proliferation and myogenic differentiation,<sup>17,35</sup> their transplant presents numerous advantages,<sup>26</sup> circumventing critical limitations of satellite cell-based cell therapy of skeletal muscle.<sup>29,31</sup> These



limitations are related to unsolved challenges presented by the harvesting of an appropriate number of fusion-competent satellite cells<sup>3</sup> and the restricted capacity of injected satellite cells to repopulate adult skeletal muscle tissue and form multinucleated muscle fibers.

MSCs may also act as a production site for secreted factors that block adipogenesis and stimulate aspects of myogenesis and tissue repair,<sup>23,32</sup> and that demonstrate a certain capacity to prevent degenerative muscle changes in the chronically torn rotator cuff.<sup>33</sup> Thus, MSC-based therapy may be an option to prevent muscle deterioration in situations when the synthetic capacity for muscle proteins is critically low,<sup>18,39</sup> such as in rotator cuff disease. This pathology is characterized by the conversion of muscle into fat tissue after a chronic tear of the rotator cuff tendon.<sup>21</sup> Recently, the injection of adipose-derived stem cells into subscapularis muscle in a rabbit model was found to improve fatty degeneration and healing of the ruptured rotator cuff 6 weeks after application in the released muscle.<sup>26</sup>

The massive degree of fatty atrophy that is characteristic of chronic tears of the rotator cuff tendon in humans is better reproduced by the experimental release of infraspinatus (ISP) tendons in sheep, compared with rodent models, by an osteotomy,<sup>14,27</sup> starting after 6 weeks and being nearly complete within 16 weeks after osteotomy. Fatty atrophy of sheep ISP muscle is accompanied by the downregulated expression of gene transcripts for myogenic processes concomitant with the upregulated expression of the adipocyte differentiation marker peroxisome proliferator-activated receptor gamma 2 (PPARG2).<sup>11,14</sup> Collectively, these molecular alterations reflect the increased area percentage of the muscle cross-sectional area being covered by lipid at the expense of muscle fibers.

The purpose of this investigation was to test the capacity of injected autologous MSCs to halt muscle degeneration through the stimulation of myogenesis and abrogation of adipogenesis in the ISP muscle after delayed tendon repair. Differences in muscle composition after tendon release and repair were compared between MSC-injected regions and noninjected controls, and we investigated the relationship between the pluripotent capacity of the implanted MSCs and the observed cellular and molecular effects.

## METHODS

### Ethics

The animal experiment was conducted with permission of the institutional review board and local federal authorities

(No. 72/2013) according to the Swiss laws of animal welfare. Animal care and surgeries were performed by veterinarians at the Animal Hospital of the University of Zurich. Sheep were housed in animal-friendly stables in groups of up to 6 animals. Pain and suffering of the animals were minimized by appropriate anesthesia, analgesia, daily monitoring of health status, and a suspension system after repair, as previously described.<sup>13</sup> Food and water were available *ad libitum*.

### Design

A total of 14 female Swiss Alpine sheep (provider, Stafflegg, Küttigen, Switzerland) were subjected to unilateral tendon release allowing for myotendinous retraction of the ISP for 16 weeks followed by repair of the tendon as previously described.<sup>13</sup> The experiment was conducted in 2 groups: Tendon repair was performed with concomitant injection of autologous MSCs and medium (group T-MSC; n = 8) or no MSC injection (group T; n = 6), with subsequent recovery for up to 6 weeks (Appendix Table A1, available in the online version of this article). Sheep were assigned to either of the 2 groups beforehand, with the intention to match the approximate age of the animals, but group T was to undergo the entire experiment before group T-MSC. MSCs were prepared from bone marrow aspirate (Appendix Figure A1, available online), labeled with fluorescent nanoparticles, and implanted in a demarcated region of ISP muscle of group T-MSC (Figure 1). Another demarcated region of ISP muscle in group T-MSC was injected with medium only. In 6 of these sheep, the experiment was terminated 6 weeks after recovery from repair. In the other 2 sheep of this group, the experiment was terminated after 2 weeks, or 2 days after repair, to descriptively assess the fate of the injected MSCs into the host tissue based on the fluorescent labeling of the MSCs. Compositional alterations in the released ISP muscle and its contralateral control were documented in anesthetized animals with a radiological method (computed tomography [CT] and magnetic resonance imaging [MRI]) immediately after tendon release, after tendon repair, and at the end of the experiment. Tissue biopsy specimens were sampled during surgery from MSC-injected, media-injected, or noninjected regions of ISP muscle for group T-MSC and anatomically comparable regions in group T (Figure 1) and subjected to biochemical characterization. Further, sampling was performed from the different regions of the excised ISP muscle and subjected to histological characterization.

\*Address correspondence to Martin Flück, PhD, Professor, Laboratory of Muscle Plasticity, Department of Orthopedics, University of Zurich, Balgrist Campus, Lengghalde 5, Zurich, 8008, Switzerland (email: martin.flueck@tutanota.com).

†Author deceased.

‡Laboratory of Muscle Plasticity, Department of Orthopedics, University of Zurich, Balgrist Campus, Zurich, Switzerland.

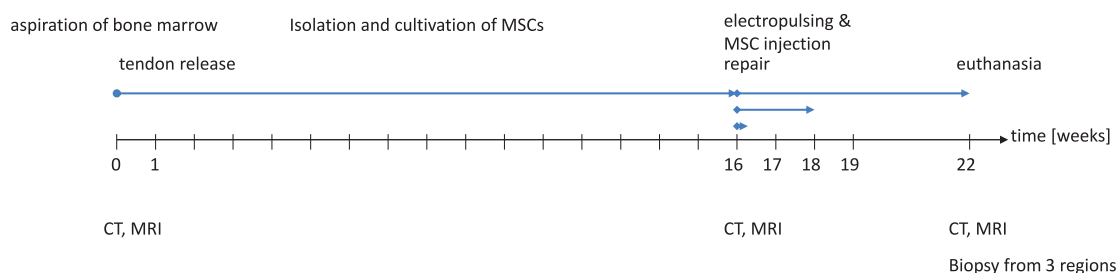
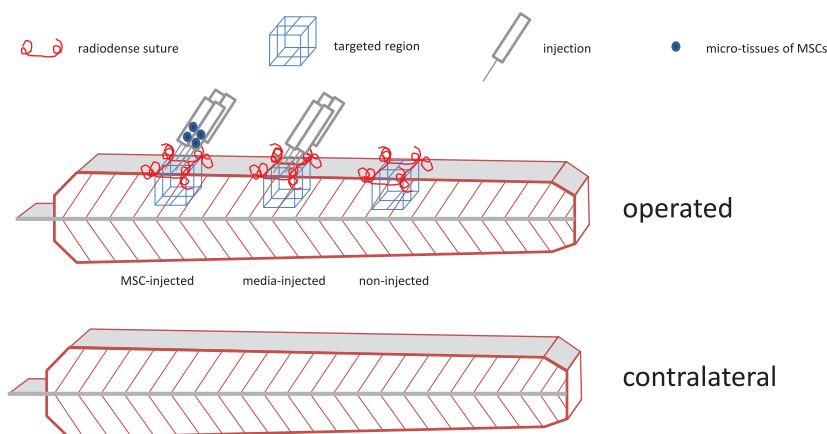
§Musculoskeletal Research Unit, Center for Applied Biotechnology and Molecular Medicine, Department of Molecular Mechanisms, Vetsuisse Faculty, University of Zurich, Zurich, Switzerland.

||Cardiology, Faculty of Sciences and Medicine, University of Fribourg, Fribourg, Switzerland.

¶University Hospital Balgrist, Department of Orthopedics, University of Zurich, Zurich, Switzerland.

Submitted May 28, 2020; accepted July 13, 2021.

One or more of the authors has declared the following potential conflict of interest or source of funding: The project was supported by a grant from RESORTHO and the Swiss National Science Foundation. AOSM checks author disclosures against the Open Payments Database (OPD). AOSM has not conducted an independent investigation on the OPD and disclaims any liability or responsibility relating thereto.

**A** Group TGroup T-MSC**B**

**Figure 1.** Overview of the intervention and sampling scheme. (A) Design of the experiment with timing of the surgical interventions and sampling and (B) location of the muscle-targeted interventions. CT, computed tomography; MRI, magnetic resonance imaging; MSC, mesenchymal stem cell.

Details of the procedures are described in the Appendix (available online).

**Tendon Release**

All operative procedures were carried out on the right shoulder of each anesthetized sheep, with the left shoulder serving as a control.<sup>13</sup> In brief, the ISP tendon was released by an osteotomy of the greater tuberosity. The tendon stump with its attached bone chip was grasped with 2 figure-of-8 stitches and wrapped in a silicon tube. Immediately after surgery, radiological measurements were made on both shoulders.

**Repair**

Radiological measurements were repeated immediately before rotator cuff repair. The ISP tendon–bone chip complex

was exposed and released from adhesions. The silicon tube was removed, and the bone chip was reattached as close as possible to its original site.

**Recovery and Sacrifice**

During the first 3 weeks of recovery after repair, we prevented animals from full weightbearing by attaching a ball to the sheep's claws and using a loose suspension belt. Before sacrifice, radiological measurements were conducted on both shoulders. Biopsy specimens (20–40 mg) were collected from the lateral aspects of the midportion of the intact contralateral ISP muscle and the different regions of the lateral aspect of the repaired ISP muscle (Figure 1B). Collected samples were immediately frozen in nitrogen-cooled isopentane.

Subsequently, the entire ISP muscles were excised, and the animals subsequently euthanized. Excised repaired

and contralateral ISP muscles were fixed for 72 hours at room temperature in 1.5 L of 4% buffered formalin. Samples ( $\sim 0.3 \times 1 \times 1$  cm in size) were collected from the demarcated regions of the repaired muscle (Figure 1B) and a corresponding region in the contralateral control.

### MSC Preparation

Starting 6 weeks before microtissue implantation, 20 mL of bone marrow was drawn from the pelvic medulla. MSCs were extracted, and the adherent cells were grown in a first seeding in 10% fetal calf serum–Dulbecco's modified Eagle medium (FCS-DMEM) (low glucose + glutamine 2 mM, 1% penicillin-streptomycin; Gibco) and then in complete medium to a density of  $5 \times 10^5$  cells in a T75 flask, as previously described.<sup>8,9</sup>

At 6 days before implantation, the cells were labeled with fluorescent nanoparticles (QTracker Cell Labeling Kit; Invitrogen, Life Technologies), seeded as  $5 \times 10^3$  cells in 25  $\mu$ L of medium per well in 60-well Terasaki plates, and grown upside down at 37°C and 5% CO<sub>2</sub> in an incubator, as previously described.<sup>24</sup> An aliquot of the cell suspension was classified by flow cytometry based on epitopes for phenotypic markers (CD29 and Stro-4, CD166, CD44, CD31, CD34, IgG1, and IgG2), and their osteogenic, chondrogenic, and/or adipogenic differentiation potential was examined by the cultivation in specific medium conditions, as previously described<sup>8,9</sup> (Appendix Figures A1 and A2, available online).

### MSC Implantation

On the day of repair surgery, for each animal, 720 microtissues were resuspended in DMEM, distributed in four 1-mL syringes, and stored in sterile conditions at 37°C until use. The resulting portions of 180 microtissues (0.9 Mio cells per 0.4 mL) were injected through 20-mm 27G needles at a depth of 2 cm in each quadrant of a  $2 \times 2$ -cm area in the lateral portion of ISP muscle that was demarcated with radiodense surgical suture. Another  $2 \times 2$ -cm region that was located more proximally, and injected accordingly with DMEM alone, was used as media control. A third region, which was only demarcated, was used as a noninjection control. Before injection, electropulsing was performed as previously described<sup>6</sup> at the lateral and medial border of the 3 demarcated regions to enhance the permeability of the extracellular matrix.<sup>30</sup>

### Radiological Assessment of Structural Muscle Changes

CT and MRI were conducted as previously established.<sup>13</sup> CT was carried out with a Somatom ART (Siemens Medical Solutions) to document musculotendinous retraction and to record the density of the muscle tissue in Hounsfield units. MRI was performed with a 3.0-T system using a dedicated receive-only extremity coil (Philips Ingenia 3T with dStream body coil solution; Philips AG) to determine muscle volume, fat, and water fraction in voxels corresponding

to the targeted regions as identified by the radiodense sutures.

### Histological Analysis

Formalin-fixed samples were processed to quantify the area percentages covered by muscle fiber types, fat and extracellular ground substance, MSCs, and the mean cross-sectional area (MCSA) and number of muscle fibers, based on the microscopic evaluation of immunochemically stained structures, and Qdot fluorescence, as described in the Appendix (available online). In addition, the overall morphology was assessed through the use of hematoxylin and eosin and Van Gieson staining of deparaffinized sections.

### Biochemical Analysis

Homogenates were prepared from paraffin-embedded blocks with a modification of a published protocol<sup>1</sup> to obtain a protein extract that was analyzed by sodium dodecyl sulfate–polyacrylamide gel electrophoresis and immunoblotting to quantify the abundance of myogenin (MyoG), tenascin-C, and PPARG2 relative to sarcomeric  $\alpha$ -actin (see the Appendix, available online).

### Statistical Analysis

Statistical analyses were carried out with SPSS (IBM SPSS Statistics 23). For anatomic variables, differences between sample points (0 weeks, 16 weeks, and 22 weeks) were assessed with a repeated-measures analysis of variance with Fisher post hoc test. The assumption of sphericity was verified with the Mauchly test. For histological and molecular variables, differences between regions (MSC-injected, media-injected, and noninjected) of the repaired muscle and contralateral side were assessed with multivariate analysis of variance. Linear relationships were assessed by Pearson correlations. Correlations were considered significant at  $P < .05$  and  $r > 0.70$ . Numerical values are expressed as mean  $\pm$  SD.

## RESULTS

### Effects of Surgery

Retraction was comparable in groups T and T-MSC, and the position of the chip relative to the original site of insertion did not differ between the groups at 6 weeks after repair (Appendix Table A1, available online). Compared with day 0, the mass of the sheep increased by 23% in group T and by 13% in group T-MSC during the 16 weeks after tendon release.

### Effects of Tendon Release on ISP Volume and Fat Fraction

At 16 weeks after tendon release, the volume of the released ISP muscle was comparably reduced in groups T

TABLE 1  
Consequences of Tendon Release and Repair on Infrapinatus Muscle Volume<sup>a</sup>

Group	Time Point	Operated Side			Contralateral Side		
		Mean ± SD	vs 0 wk	vs 16 wk	Mean ± SD	vs Operated	vs 16 wk
T	0 wk	166.2 ± 14.2			162.0 ± 16.9	.054	
T	16 wk	130.3 ± 18.3	<.001		176.8 ± 16.0	<.001	.001
T	22 wk	115.0 ± 14.7	<.001	.011	172.0 ± 21.2	<.001	.025 .034
T-MSC	0 wk	184.7 ± 34.0			186.3 ± 36.2	.403	
T-MSC	16 wk	136.7 ± 25.2	<.001		181.5 ± 35.5	<.001	.148
T-MSC	22 wk	134.3 ± 22.1	<.000	.646	181.2 ± 35.1	<.001	.203 .869

<sup>a</sup>Infrapinatus muscle volume (in mL) was estimated by magnetic resonance imaging–based volumetry in groups T (n = 6) and T-MSC (n = 6) at the different time points. Group T, tendon repair without injection of autologous MSCs; T-MSC, tendon repair with injection of autologous MSCs.

TABLE 2  
Consequences of Tendon Release and Repair on Fat Content<sup>a</sup>

Group	Time Point	Operated Side			Contralateral Side		
		Mean ± SD	vs 0 wk	vs 16 wk	Mean ± SD	vs Operated	vs 16 wk
<b>Fat fraction, % (MRI)</b>							
T	0 wk	7.4 ± 2.3			7.7 ± 1.9	.272	
T	16 wk	48.8 ± 5.1	<.001		12.0 ± 2.9	<.001	.147
T	22 wk	60.5 ± 6.8	<.001	.001	13.7 ± 2.7	<.001	.046 .104
T-MSC	0 wk	9.8 ± 1.8			10.1 ± 1.9	.347	
T-MSC	16 wk	53.4 ± 9.4	<.001		11.8 ± 1.9	<.001	.132
T-MSC	22 wk	53.9 ± 10.4	<.001	.843	12.6 ± 3.4	<.001	.191 .554
<b>Hounsfield units (CT)</b>							
T	0 wk	63.5 ± 7.1			64.0 ± 5.1	.814	
T	16 wk	25.7 ± 10.5	.000		63.5 ± 6.7	.000	.870
T	22 wk	11.2 ± 12.5	.000	.029	58.7 ± 4.8	.000	.068 .070
T-MSC	0 wk	61.4 ± 7.0			60.4 ± 7.9	.261	
T-MSC	16 wk	25.9 ± 13.6	.001		56.7 ± 5.4	.000	.164
T-MSC	22 wk	18.3 ± 11.3	.000	.008	52.4 ± 7.1	.000	.057 .042

<sup>a</sup>Fat fraction (%) and Hounsfield units of infrapinatus muscle as assessed by magnetic resonance imaging (MRI) and computed tomography (CT) in groups T (n = 6) and T-MSC (n = 6) at the different time points. Repeated-measures analysis of variance with Fisher post hoc test. Group T, tendon repair without injection of autologous MSCs; T-MSC, tendon repair with injection of autologous MSCs.

and T-MSC (–22% vs –26%, respectively) (Table 1). Fat fraction in the released ISP muscle was comparably increased in groups T and T-MSC (from 7% to 49% and from 10% to 53%, respectively) (Table 2). The values for the Hounsfield units in the repaired muscle were comparably reduced in both groups.

#### Effects of MSC Implantation on ISP Volume and Fat Fraction 6 Weeks After Repair

In group T, the repaired ISP muscle demonstrated a further increase in fat fraction to 61% during the 6 weeks after repair, while its volume was further reduced to 115 cm<sup>3</sup> (Tables 1 and 2). The contralateral muscle demonstrated a slight reduction in volume and increase in fat fraction.

In group T-MSC, the fat fraction ( $P = .843$ ) and volume of ISP muscle ( $P = 0.646$ ) remained constant during the 6 weeks after repair, as also observed for the contralateral

muscle (Tables 1 and 2). The alterations in fat fraction (+24.0% vs +0.9%) and volume of ISP muscle (–11.7% vs –1.8%) during the 6 weeks after repair differed between groups T and T-MSC ( $P = .009$  and  $.069$ , respectively; Figure 2, A and B). As shown in Figure 2C, changes in fat mass were similar in both groups; fat-free mass was reduced in the repaired muscle of group T and was attenuated in group T-MSC (–29.2% vs –4.8%; Figure 2D). CT-based measurements demonstrated a trend for a lower degree of alteration in Hounsfield units for group T-MSC than for group T (Appendix Figure A3, available online).

#### Effects of MSC Implantation on the Composition of ISP Muscle 6 Weeks After Repair

At 6 weeks after implantation, fluorescent nanoparticle–positive structures were detected in the MSC-injected region and, as expected, were absent in the media-injected

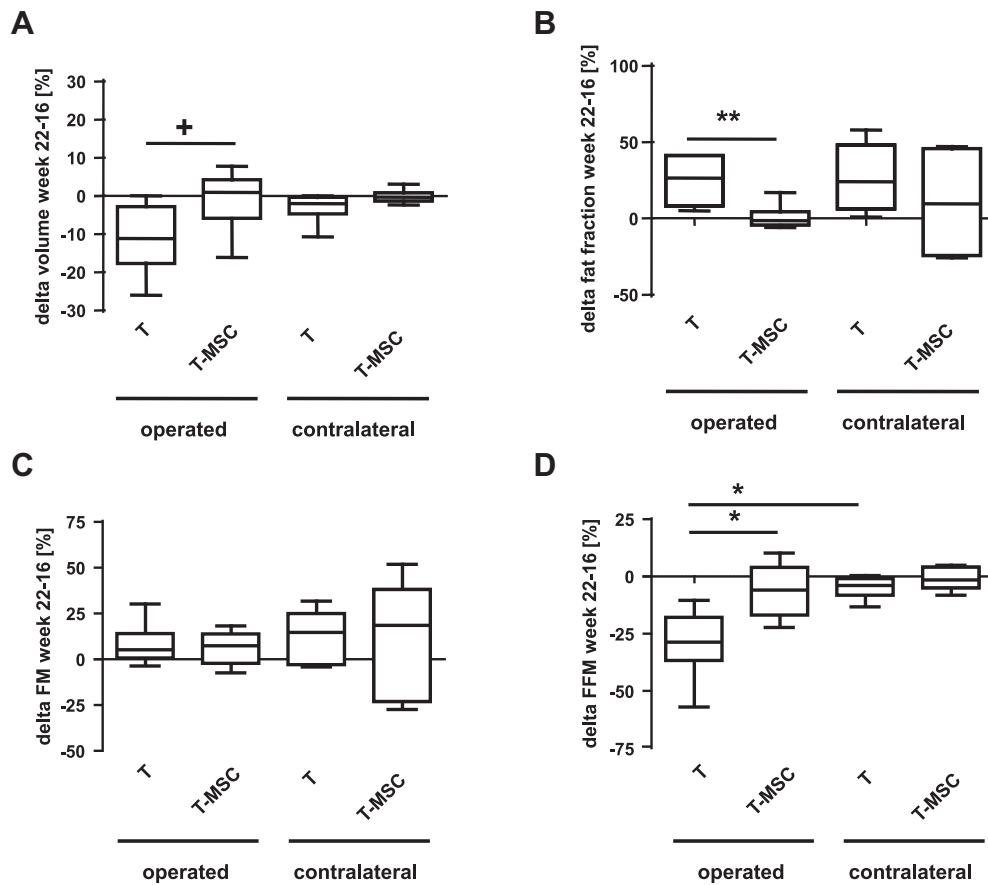


**Figure 2.** Influence of stem cell injection on changes in muscle volume and fat content after repair. Box-whisker plots of the changes in (A) volume, (B) fat fraction, (C) fat mass (FM), and (D) fat-free mass (FFM) in the repaired infraspinatus muscle and its contralateral control at 6 weeks after repair in groups T and T-MSC. +  $P < .10$ , \*  $P < .05$ , and \*\*  $P < .01$  for the indicated comparison. Analysis of variance with Fisher post hoc test. MST, mesenchymal stem cell.

region. In total, 11% of the sampled tissue in the MSC-injected region was positive for fluorescence. Fluorescence-positive structures appeared as single cells, or granuloma-like clusters, between muscle fiber bundles (Figure 3). Most of the fluorescence-positive cell structures had a diameter  $<10 \mu\text{m}$ , whereas 2.5% of the fluorescence-positive structures had a diameter  $>20 \mu\text{m}$  (Appendix Table A2, available online).

Radiologically, over the entire MSC-injected region, the water fraction was increased compared with the media-injected region of the MSC-injected ISP muscle and compared with the noninjected regions of ISP muscle from group T (Appendix Figure A4, available online). Histological evidence revealed deterioration of the local tissue structure by MSC injection (Figures 3 and 4A).

### Regional Effects of MSC Injection on the Cellular Composition of Repaired ISP Muscle

The cellular composition was quantified at the periphery of the injected regions of the ISP muscle at 6 weeks after repair: With respect to connective tissue in group T-MSC,

the area percentage of fat in the media- and MSC-injected regions was higher than in the noninjected region of the repaired ISP muscle in group T-MSC (Figure 4B). Conversely, the portion of the connective tissue that was attributable to the extracellular ground substance was 17.2% lower in the MSC-injected region than the noninjected region (fractions of 0.58 vs 0.76, respectively;  $P = .022$ ).

When we compared the noninjected region between groups T-MSC and T, the area percentage of fat was lower in the noninjected region of ISP muscle in group T-MSC than in group T (8.5% vs 19.6%, respectively;  $P = .018$ ) (Figure 4B). Conversely, the area percentage of extracellular ground substance in the noninjected region, was higher in group T-MSC compared with group T (25.5% vs 20.1%, respectively;  $P = .007$ ). Over all assessed regions, the area percentage of fat correlated negatively with the MRI-based measurements of water fraction ( $r = -0.722$ ;  $P = 7 \times 10^{-7}$ ).

In the muscle fiber compartment, the MSCA of muscle fibers irrespective of their type was lower in the MSC-injected than the media-injected region ( $-1172.0 \mu\text{m}^2$ ;  $P = .032$ ) (Appendix Table A3, available online). Fiber MSCA

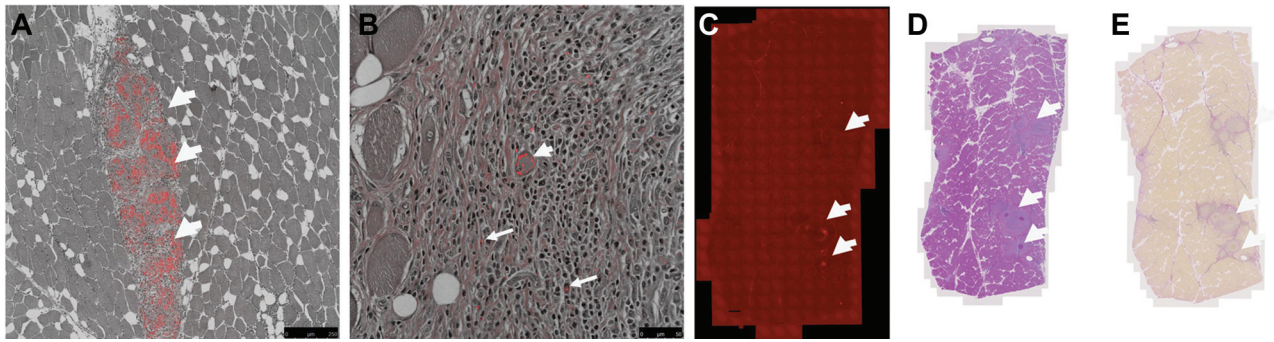


**Figure 3.** Fluorescent nanoparticle–positive cells in the injected muscles. Images of a microscopic field with detection of fluorescence in infraspinatus muscle (A) 2 days and (B) 6 weeks after injection of mesenchymal stem cells and repair. Fluorescence-positive structures contain red dots. Dense spherical structures (resembling granulomas, thick arrows) and fluorescence-positive single cells (thin arrows) are detected. A structure resembling a small muscle fiber (ie, myotube) is indicated with an arrowhead. Bar indicates 250  $\mu\text{m}$ . (C–E) Full scans of consecutive cross sections from a stem cell–injected area 6 weeks following stem cell injection after (C) visualization of the Q-tracker signal, (D) hematoxylin and eosin staining, and (E) Van Gieson staining.

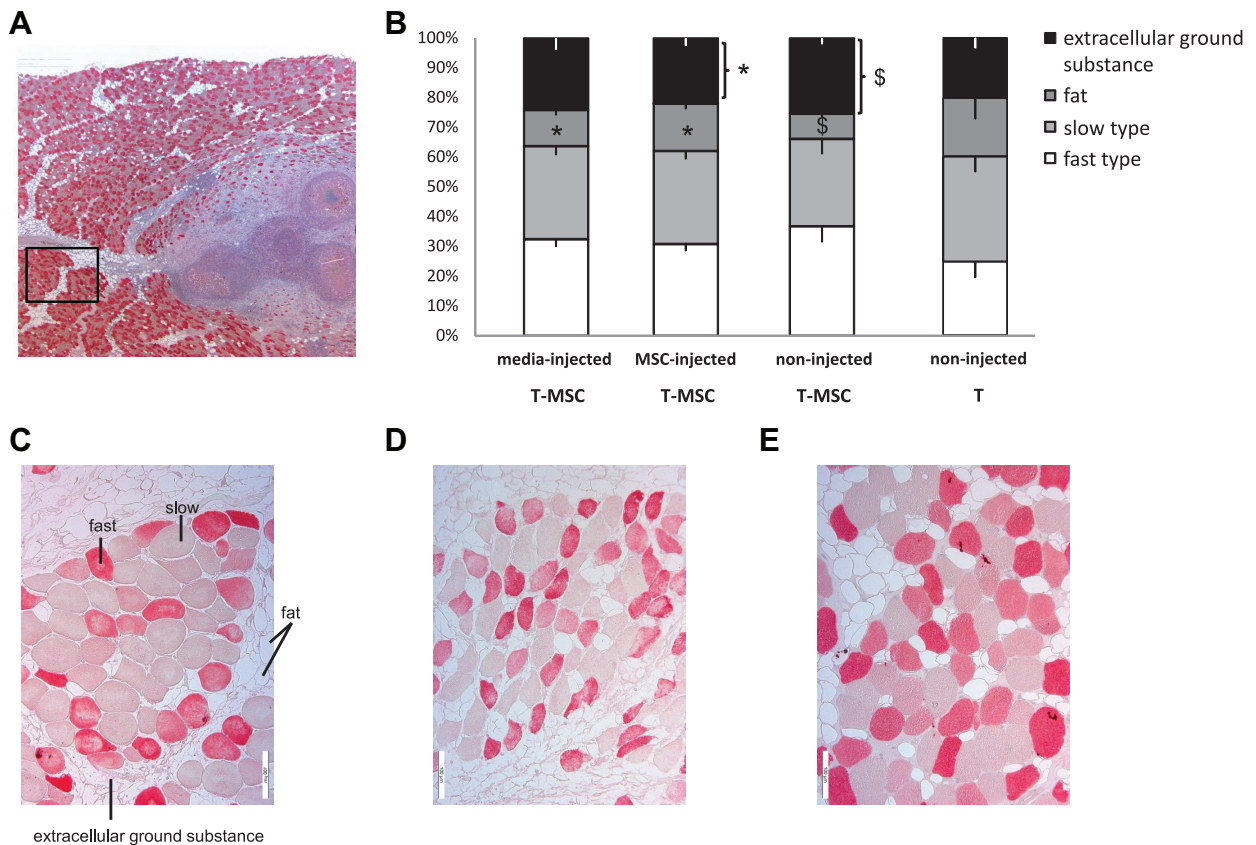


**Figure 4.** Cellular composition in mesenchymal stem cell (MSC)–injected regions of repaired infraspinatus (ISP) muscle. (A) Microscopic image of stained muscle fibers in MSC–injected region of a repaired ISP muscle from group T-MSC. The rectangle depicts an exemplary microscopic field at the periphery of the injected region, which qualified for the determination of its cellular composition because it was situated outside a granuloma. (B) Bar graph of the area percentage of slow type fibers, fast type fibers, fat, and extracellular ground substance in different regions of ISP muscle from groups T and T-MSC 6 weeks after repair.  $*P < .05$  for the difference compared with the noninjected region in group T-MSC.  $^{\$}P < .05$  for the difference compared with the noninjected region in group T. Analysis of variance with Fisher post hoc test. Curly bracket (}) indicates the portion of connective tissue composed of extracellular ground substance. (C–E) Microscopic images of stained muscle fibers in MSC–injected region (C), noninjected region (D), and media–injected region (E), in an ISP muscle from group T-MSC.

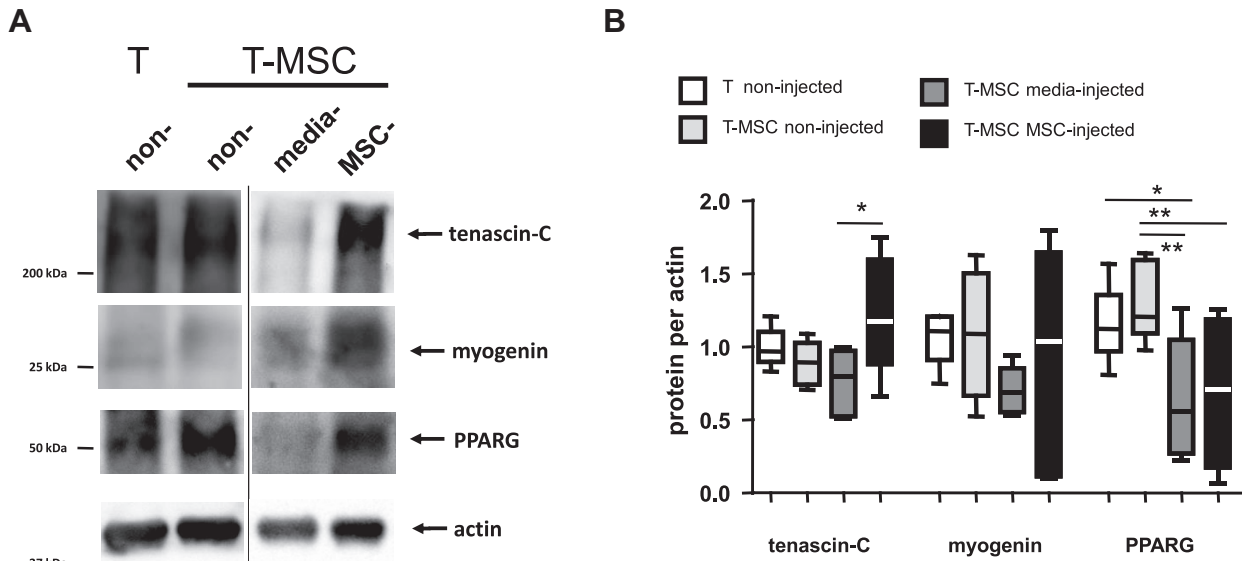


**Figure 5.** Protein expression in injected muscle areas. (A) Immunoblot showing the detected proteins in noninjected, media-injected, and mesenchymal stem cell (MSC)-injected areas of the same muscle of group T-MSC and a noninjected area of group T at 6 weeks after repair. The position of the respectively detected proteins relative to molecular size markers is indicated with an arrow. Blots that were run in separate experiments are separated by a line. (B) Box-whisker plot of median, 25%-75% CI (box), and minimum/maximum (top/bottom) for the assessed proteins. \* $P < .05$  and \*\* $P < .01$  for the indicated comparison. Analysis of variance with Fisher post hoc test. PPARG 2, peroxisome proliferator-activated receptor gamma 2.

tended to be 28.7% larger in the media-injected region than in the noninjected region ( $+ 955.8 \mu\text{m}^2$ ;  $P = .077$ ). For the noninjected region, the MCSA of muscle fibers did not differ between groups T and T-MSC (Appendix Table A3, available online). We noted tendencies for a reduced number of muscle fibers per square micrometer (ie, frequency of muscle fibers) in the media-injected region compared with the MSC-injected and noninjected regions (Appendix Table A3, available online).

### Effects of MSC Injection and Repair on Levels of Protein Markers of Myogenesis and Adipogenesis

In the noninjected region of ISP muscle, the sarcomeric actin-related expression levels of the 3 assessed proteins, tenascin-C, MyoG, and PPARG, were similar between groups T and T-MSC at 6 weeks after repair.

For group T-MSC, the expression level of the adipogenic marker PPARG was 2-fold lower in the media-injected and MSC-injected regions than the noninjected muscle region (Figure 5). The tenascin-C level was 59% higher in the MSC-injected region than in the media-injected region. The MyoG levels did not differ between any of the muscle regions but were correlated with the levels of PPARG ( $r = 0.565$ ;  $P = .004$ ).

### Relationships to Stem Cell Dose

In the MSC-injected regions, we found significant, positive correlations between the fluorescent signal, the frequency of muscle fibers ( $r = 0.745$ ;  $P = .005$ ), and the tenascin-C

protein level ( $r = 0.853$ ;  $P < .001$ ). The lipogenic potential of the MSC preparations also correlated with the tenascin-C protein levels ( $r = 0.912$ ;  $P = .011$ ) and the frequency of muscle fibers ( $r = 0.865$ ;  $P = .026$ ). Tenascin-C protein levels correlated negatively with the levels of the markers for the hematopoietic (CD34;  $r = -0.860$ ;  $P = .028$ ) and endothelial (CD31;  $r = -0.884$ ;  $P = .019$ ) phenotypes of the MSC preparation and positively with the frequency of muscle fibers ( $r = 0.747$ ;  $P = .005$ ). MyoG levels negatively correlated with the levels of the marker of activated stem cells (Stro-4) in the MSC preparation ( $r = -0.868$ ;  $P = .025$ ).

### DISCUSSION

Therapy based on stem cells, and especially MSCs, has been proposed as a possible venue to enhance the regenerative capacity of musculoskeletal tissues, especially in rotator cuff disease atrophy.<sup>25,26,34,36,38</sup> Currently, it is difficult to give recommendations for or against the use of stem cells to treat rotator cuff tears.<sup>16</sup> Specifically, the influence and efficiency of stem cell-based therapy on muscle degeneration in rotator cuff disease are poorly understood because previous investigations targeted MSC injection to bone or tendon structures and/or used small laboratory species<sup>25,26</sup> that are not useful for developing surgical procedures and stem cell isolation in humans.<sup>22,28</sup> To provide insight into the potential of MSCs to halt muscle-to-fat conversion in rotator cuff disease, we characterized molecular, microscopic, and macroscopic effects of implanting bone marrow-derived microtissues of MSCs

into a detached rotator cuff muscle of a large animal model (sheep) that reproduces the massive degree of lipid accumulation and atrophy seen in humans.<sup>14</sup> The use of bone marrow-derived rather than adipose-derived MSCs was motivated by preparatory work establishing a protocol for the quantitative isolation of abundant MSCs that retains their capacity to differentiate into the cell types of skeletal muscle,<sup>8,9</sup> including the myogenic lineage that is lost in a detached rotator cuff muscle after the release, or tear, of its tendon.<sup>11,12</sup>

The main finding of this investigation was that a single administration of microtissues of bone marrow-derived MSCs stopped the atrophy and increase in fat fraction of the chronically retracted ISP muscle after repair in sheep (Figure 2). The mitigation of fatty atrophy was explained by the prevention of a decrease in fat-free mass during the 6 weeks after repair in the MSC-treated ISP muscle. The reduced area percentage of fat and concomitant increase in extracellular ground substance in regions of ISP muscle (Figure 4; Appendix Table A3, available online) are in line with previously reported effects of MSC injection: promotion of extracellular matrix deposition in muscle tissue<sup>7</sup> and reduced fat content in rabbit subscapularis muscle after tendon repair.<sup>26</sup> The influence of MSC treatment in noninjected regions of ISP muscle suggests a paracrine action of the injected stem cells on rotator cuff muscle that involves secreted factors that can block adipogenesis.<sup>23,32,33</sup> In contrast, the M CSA of muscle fibers in the noninjected muscle regions did not differ between groups T and T-MSC. Collectively, our findings suggest that hypertrophy of the connective tissue, rather than the muscle fiber compartment, explained the mitigated loss in fat-free mass of sheep ISP muscle during the 6 weeks after tendon repair with MSC treatment (Figure 2).

The increased area percentage of fat in regions of the repaired ISP muscles that were treated by media adjuvant (ie, DMEM) alone, or in combination with MSCs, indicates that lipid accumulation was not prevented at the site of injection. This observation is in line with the augmentation of fat cell content in rabbit subscapularis muscle by control injections with saline (ie, 63% vs 18%).<sup>26</sup> The concomitant elevation of the water fraction (Appendix Figure A4, available online) and the lowered levels of the adipogenic master regulator PPARG<sup>14</sup> (Figure 5) imply that the local deterioration of muscle structure at the site of media and MSC injection comprises swelling and a reduced PPARG protein abundance. PPARG protein levels correlate positively with the area percentage of the extracellular ground substance, rather than lipid, in released sheep ISP muscle,<sup>12</sup> indicating that the regional deterioration of muscle composition with media injection is connected to the downregulation of PPARG protein and its action on extracellular matrix synthesis.<sup>20</sup>

The increased levels of the extracellular protein tenascin-C and the decreased area percentage of extracellular ground substance in the MSC-injected region (Figures 4B and 5B) are signposts for the remodeling of the extracellular environment and heightened muscle fiber regeneration due to the injected MSCs.<sup>10,34,37</sup> This interpretation is

supported by the tentatively elevated muscle fiber frequency in the MSC-injected compared with the media-injected regions ( $P = .09$ ), the identification of Q tracker-labeled cellular structures that had the appearance small muscle fibers (Figure 3B; Appendix Table A2, available online), and the correlation between tenascin-C levels and the muscle fiber frequency.<sup>15</sup> Thereby, the tenascin-C levels correlated with parameters indicating the dose and differentiation potential of the injected MSC preparation: that is, the signal of the Q-tracker fluorescent label, the lipogenic potential, and hematopoietic and endothelial markers. Collectively, our observations emphasize that a limited degree of myogenic reaction is set in motion within the MSC-injected region of repaired ISP muscle, which is ameliorated with a reduced lipogenic potential of the injected MSCs preparation.

We estimate that the ISP region being injected with 0.9 Mio MSCs corresponds to ~5% of the total muscle volume (8 mL/173 mL). The observed macroscopic and microscopic effects highlight the efficacy of injecting a relatively small dose of bone marrow-derived MSCs during reconstructive tendon surgery to halt the progression of fatty atrophy of a retracted rotator cuff muscle. Bone marrow-derived MSC preparations thus appear suitable as biological agents during tendon repair surgery in humans to mitigate the degeneration of a previously torn rotator cuff muscle that otherwise may continue into the recovery phase (reviewed by Flück et al<sup>11</sup> and Osti et al<sup>27</sup>). Incidentally, an elevated fiber M CSA indicated that media injection alone produced a regional anabolic reaction that was blunted by the inclusion of MSCs (Appendix Table A3, available online). Future research may explore how potential bottlenecks, such as the time-intensive preparation of autologous microtissues, can be resolved and may address the specific roles of media-adjuvant and MSC-secreted factors to block adipogenesis and stimulate muscle regeneration.

Our study bears a number of limitations. One such limitation is the extent to which injected microtissues of MSCs can contribute to muscle regrowth because the enveloping basement membrane critically affects the regenerative capacity of transplanted muscle stem cells.<sup>4</sup> We applied electropulsing to enhance the permeability of the extracellular matrix, as previously described.<sup>30</sup> However, most of the fluorescent signal was retained in granuloma-like structure in the injected region at 6 weeks after injection (Figure 3), indicating that electropulsing did not appear to promote the migration of the injected MSCs or muscle fiber damage.<sup>6</sup> The formation of granulation tissue with a fibrous capsule in the MSC-injected region possibly reflects an adaptive immune response, as shown formerly with the incorporation of biological components of allogenic or xenogenic origin.<sup>2</sup> Future investigations are required to address whether the tissue response to the injection of autologous MSCs is related to the toxicity of the concurrent injection of the fluorescent nanoparticles.<sup>19</sup> The recovery phase of 6 weeks was possibly too short to test whether the injected MSCs can themselves contribute to the formation of muscle tissue by growing into full-sized muscle fibers.<sup>5</sup> Further, certain group differences existed for

body mass at baseline and the alterations of body mass, but not the percentage changes of ISP volume, during the first 16 weeks after tendon release, emphasizing different systemic reactions before MSC-based therapy was administered. Last, the experimental model to produce muscle retraction by osteotomy, although representing fatty atrophy,<sup>14</sup> does not exactly match the situation of rotator cuff disease in humans that is due to tearing of the tendon and that may induce confounding degenerative processes.

## CONCLUSION

The injection of viable MSCs jointly with electropulsing was technically feasible in large animals and blunted the progression of fat accumulation and atrophy in rotator cuff muscle after tendon repair via an unexplained paracrine pathway, which involved an expansion of the extracellular ground substance and an increased tissue water content. Within the directly targeted region, the injection of MSCs introduced tenascin C–associated myogenic reactions while preserving downregulation of the adipocyte differentiation marker PPAR $\gamma$ , but not the regional muscle fiber hypertrophy, seen with adjuvant injection alone.

## ACKNOWLEDGMENT

The authors greatly appreciate the supply of antibodies by Prof Andrew Zannettino, University of Adelaide, Australia. The authors thank Drs Paola Valdivieso and Severin Ruoss and Céline Ferrié, MSc, for assisting in the histological analysis. The project was supported by a grant from RESORTHO and the Swiss National Science Foundation.

## Availability of Data and Materials

The data sets generated and/or analyzed during the current study are available in the Mendeley data repository: Flück, M. Transplantation of autologous mesenchymal stem cells during repair of detached rotator cuff muscle in sheep. Published in 2019. <http://dx.doi.org/10.17632/hwdxv5dvhk.1>

## ORCID iDs

Martin Flück  <https://orcid.org/0000-0002-0479-7243>

Christian Gerber  <https://orcid.org/0000-0002-4624-8285>

## REFERENCES

- Addis MF, Tanca A, Pagnozzi D, et al. Generation of high-quality protein extracts from formalin-fixed, paraffin-embedded tissues. *Proteomics*. 2009;9(15):3815-3823.
- Anderson JM, Rodriguez A, Chang DT. Foreign body reaction to biomaterials. *Semin Immunol*. 2008;20(2):86-100.
- Asakura A, Seale P, Girgis-Gabardo A, Rudnicki MA. Myogenic specification of side population cells in skeletal muscle. *J Cell Biol*. 2002;159(1):123-134.
- Boldrin L, Neal A, Zammit PS, Muntoni F, Morgan JE. Donor satellite cell engraftment is significantly augmented when the host niche is preserved and endogenous satellite cells are incapacitated. *Stem Cells*. 2012;30(9):1971-1984.
- Dawson JL, Kanczler J, Tare R, Kassem M, Oreffo RO. Concise review: bridging the gap: bone regeneration using skeletal stem cell-based strategies—where are we now? *Stem Cells*. 2014;32(1):35-44.
- Eigeldinger-Berthou S, Buntschu P, Flück M, et al. Electric pulses augment reporter gene expression in the beating heart. *J Gene Med*. 2012;14(3):191-203.
- El-Said MM, Emile SH. Comment on “A new method for treating fecal incontinence by implanting stem cells derived from human adipose tissue: preliminary findings of a randomized double-blind clinical trial.” *Stem Cell Res Ther*. 2018;9(1):115.
- Emmert MY, Wolint P, Wickboldt N, et al. Human stem cell-based three-dimensional microtissues for advanced cardiac cell therapies. *Biomaterials*. 2013;34(27):6339-6354.
- Emmert MY, Wolint P, Winkhofer S, et al. Transcatheter based electromechanical mapping guided intramyocardial transplantation and in vivo tracking of human stem cell based three dimensional microtissues in the porcine heart. *Biomaterials*. 2013;34(10):2428-2441.
- Flück M, Mund SI, Schittny JC, Klossner S, Durieux AC, Giraud MN. Mechano-regulated tenascin-C orchestrates muscle repair. *Proc Natl Acad Sci U S A*. 2008;105(36):13662-13667.
- Flück M, Ruoss S, Mohl CB, et al. Genomic and lipidomic actions of nandrolone on detached rotator cuff muscle in sheep. *J Steroid Biochem Mol Biol*. 2017;165(pt B):382-395.
- Flück M, Valdivieso P, Ruoss S, et al. Neurectomy preserves fast fibers when combined with tenotomy of infraspinatus muscle via upregulation of myogenesis. *Muscle Nerve*. 2019;59(1):100-107.
- Gerber C, Meyer DC, Flück M, Benn MC, von Rechenberg B, Wieser K. Anabolic steroids reduce muscle degeneration associated with rotator cuff tendon release in sheep. *Am J Sports Med*. 2015;43(10):2393-2400.
- Gibbons MC, Singh A, Engler AJ, Ward SR. The role of mechanobiology in progression of rotator cuff muscle atrophy and degeneration. *J Orthop Res*. 2018;36(2):546-556.
- Giddings CJ, Neaves WB, Gonyea WJ. Muscle fiber necrosis and regeneration induced by prolonged weight-lifting exercise in the cat. *Anat Rec*. 1985;211(2):133-141.
- Goldenberg BT, Lacheta L, Dekker TJ, Spratt JD, Nolte PC, Millett PJ. Biologics to improve healing in large and massive rotator cuff tears: a critical review. *Orthop Res Rev*. 2020;12:151-160.
- Grabowska I, Streminska W, Janczyk-Ilach K, et al. Myogenic potential of mesenchymal stem cells—the case of adhesive fraction of human umbilical cord blood cells. *Curr Stem Cell Res Ther*. 2013;8(1):82-90.
- Gulotta LV, Kovacevic D, Packer JD, Deng XH, Rodeo SA. Bone marrow-derived mesenchymal stem cells transduced with scleraxis improve rotator cuff healing in a rat model. *Am J Sports Med*. 2011;39(6):1282-1289.
- Hsieh SC, Wang FF, Lin CS, Chen YJ, Hung SC, Wang YJ. The inhibition of osteogenesis with human bone marrow mesenchymal stem cells by CdSe/ZnS quantum dot labels. *Biomaterials*. 2006;27(8):1656-1664.
- Kim HJ, Kim MY, Jin H, et al. Peroxisome proliferator-activated receptor  $\delta$  regulates extracellular matrix and apoptosis of vascular smooth muscle cells through the activation of transforming growth factor- $\beta$ 1/Smad3. *Circ Res*. 2009;105(1):16-24.
- Laron D, Samagh SP, Liu X, Kim HT, Feeley BT. Muscle degeneration in rotator cuff tears. *J Shoulder Elbow Surg*. 2012;21(2):164-174.
- Lebaschi A, Deng XH, Zong J, et al. Animal models for rotator cuff repair. *Ann N Y Acad Sci*. 2016;1383(1):43-57.
- Lee RH, Oh JY, Choi H, Bazhanov N. Therapeutic factors secreted by mesenchymal stromal cells and tissue repair. *J Cell Biochem*. 2011;112(11):3073-3078.
- Mirsaidi A, Tiaden AN, Richards PJ. Preparation and osteogenic differentiation of scaffold-free mouse adipose-derived stromal cell microtissue spheroids (ASC-MT). *Curr Protoc Stem Cell Biol*. 2013;27:2B.5.1-2B.5.12.

25. Morton-Gonzaba N, Carlisle D, Emukah C, Chorath K, Moreira A. Mesenchymal stem cells and their application to rotator cuff pathology: a meta-analysis of pre-clinical studies. *Osteoarthritis Cartilage Open*. 2020;2(2):100047.
26. Oh JH, Chung SW, Kim SH, Chung JY, Kim JY. 2013 Neer Award: Effect of the adipose-derived stem cell for the improvement of fatty degeneration and rotator cuff healing in rabbit model. *J Shoulder Elbow Surg*. 2014;23(4):445-455.
27. Osti L, Buda M, Del Buono A. Fatty infiltration of the shoulder: diagnosis and reversibility. *Muscles Ligaments Tendons J*. 2013;3(4):351-354.
28. Pigeau GM, Csaszar E, Dulgar-Tulloch A. Commercial scale manufacturing of allogeneic cell therapy. *Front Med*. 2018;5:233.
29. Rodrigues M, Griffith LG, Wells A. Growth factor regulation of proliferation and survival of multipotential stromal cells. *Stem Cell Res Ther*. 2010;1(4):32.
30. Rols MP. Electroporation, a physical method for the delivery of therapeutic molecules into cells. *Biochim Biophys Acta*. 2006;1758(3):423-428.
31. Sambasivan R, Tajbakhsh S. Adult skeletal muscle stem cells. *Results Probl Cell Differ*. 2015;56:191-213.
32. Sassoli C, Zecchi-Orlandini S, Formigli L. Trophic actions of bone marrow-derived mesenchymal stromal cells for muscle repair/regeneration. *Cells*. 2012;1(4):832-850.
33. Seivivas N, Teixeira FG, Portugal R, et al. Mesenchymal stem cell secretome: a potential tool for the prevention of muscle degenerative changes associated with chronic rotator cuff tears. *Am J Sports Med*. 2016;45(1):179-188.
34. Shi X, Garry DJ. Muscle stem cells in development, regeneration, and disease. *Genes Dev*. 2006;20(13):1692-1708.
35. Smolina NA, Davydova A, Shchukina IA, et al. Comparative assessment of different approaches for obtaining terminally differentiated muscle cells. Article in Russian. *Tsitologiya*. 2014;56(4):291-299.
36. Tedesco FS, Dellavalle A, Diaz-Manera J, Messina G, Cossu G. Repairing skeletal muscle: regenerative potential of skeletal muscle stem cells. *J Clin Invest*. 2010;120(1):11-19.
37. Tierney MT, Gromova A, Sesillo FB, et al. Autonomous extracellular matrix remodeling controls a progressive adaptation in muscle stem cell regenerative capacity during development. *Cell Rep*. 2016;14(8):1940-1952.
38. Valencia Mora M, Ruiz Iban MA, Diaz Heredia J, et al. Stem cell therapy in the management of shoulder rotator cuff disorders. *World J Stem Cells*. 2015;7(4):691-699.
39. Vilquin JT, Catelain C, Vauchez K. Cell therapy for muscular dystrophies: advances and challenges. *Curr Opin Organ Transplant*. 2011;16(6):640-649.
40. Yin H, Price F, Rudnicki MA. Satellite cells and the muscle stem cell niche. *Physiol Rev*. 2013;93(1):23-67.